

**CLASSIFICATION CANCELLED**

Copy /  
RM SL53E11a

REC'D MAY 25 1953

Authority: NASA PUBLICATIONS  
ANNOUNCEMENTS NO. 27  
Date 9/4/50 By [Signature]

Source of Acquisition  
CASI Acquired

RESTRICTION CANCELLED  
UNCLASSIFIED UNAVAILABLE Restriction/Classification Cancelled



# RESEARCH MEMORANDUM

for the

U. S. Air Force

DRAG AND LONGITUDINAL TRIM AT LOW LIFT OF THE NORTH AMERICAN

YF-100A AIRPLANE AT MACH NUMBERS FROM 0.76 TO 1.77

AS DETERMINED FROM THE FLIGHT TEST OF A

0.11-SCALE ROCKET MODEL

By Willard S. Blanchard, Jr.

Langley Aeronautical Laboratory  
Langley Field, Va.

RESTRICTION CANCELLED  
UNCLASSIFIED UNAVAILABLE Restriction/Classification Cancelled

This material contains information affecting the National Defense of the United States within the meaning of the espionage laws, Title 18, U.S.C., Secs. 793 and 794, the transmission or revelation of which in any manner to an unauthorized person is prohibited by law.

## NATIONAL ADVISORY COMMITTEE FOR AERONAUTICS

WASHINGTON

4 1953

**CLASSIFICATION CANCELLED**  
UNCLASSIFIED UNAVAILABLE  
**CONFIDENTIAL**

**FILE COPY**

To be returned to  
the files of the National  
Advisory Committee  
for Aeronautics  
Washington, D. C.

16

Authority: NASA PUBLICATIONS  
ANNOUNCEMENTS NO. 27  
Date 9/4/50 By [Signature]

RESEARCH MEMORANDUM

for the

U. S. Air Force

DRAG AND LONGITUDINAL TRIM AT LOW LIFT OF THE NORTH AMERICAN

YF-100A AIRPLANE AT MACH NUMBERS FROM 0.76 TO 1.77

AS DETERMINED FROM THE FLIGHT TEST OF A

0.11-SCALE ROCKET MODEL

By Willard S. Blanchard, Jr.

SUMMARY

Drag and longitudinal trim at low lift of the North American YF-100A airplane at Mach numbers from 0.76 to 1.77 as determined from the flight test of a 0.11-scale rocket model are presented herein. Also included are some longitudinal stability and some qualitative pitch-damping data.

The subsonic external-drag-coefficient level was about 0.012, and the supersonic level was about 0.043. The drag rise occurred at a Mach number of 0.95. The longitudinal trim change at low lift consisted basically of a mild nose-up tendency at a Mach number of 0.90. An indication of wing flutter was present at Mach numbers from 0.95 to 1.11. However, the full-scale airplane wing has approximately twice the scaled first-bending frequency as the model tested and, hence, will probably be free of this type of flutter. The aerodynamic-center location was 71 percent behind the leading edge of the mean aerodynamic chord at a Mach number of 1.03 and 62 percent at a Mach number of 1.74. Qualitative measurement of damping in pitch indicates that at low lift coefficients damping will be low at a Mach number of 1.03.

INTRODUCTION

An investigation of the drag and longitudinal trim at low lift of 0.11-scale rocket models of the North American YF-100A airplane is being

**CLASSIFICATION CANCELLED**

conducted by the Langley Pilotless Aircraft Research Division at the request of the U. S. Air Force. The North American YF-100A is a swept-wing jet-propelled fighter-type airplane with nose inlet and is designed to fly at supersonic speeds. The model used in the test reported herein was of an interim version of the airplane with the horizontal tail slightly above the wing chord extended. The nose inlet was replaced on the model by a pointed fairing.

The primary purpose of this test was to obtain drag and longitudinal-trim data for the complete clean configuration at low lift. In addition to drag and trim, however, some longitudinal stability and damping data were obtained through analyses of pitch disturbances created by sustainer motor burnout and by two pulse rockets.

## SYMBOLS

M	free-stream Mach number
R	Reynolds number based on mean aerodynamic chord
W	model weight, lb
$\bar{c}$	mean aerodynamic chord, 1.245 ft
q	free-stream dynamic pressure, lb/sq ft
S	model wing area (leading and trailing edges extended to fuselage center line), 4.56 sq ft
$C_C$	chord-force coefficient, $\frac{\text{Chord force}}{qS}$
$C_D$	drag coefficient, $\frac{\text{Drag}}{qS}$
$C_N$	normal-force coefficient, $\frac{\text{Normal force}}{qS}$
$C_L$	lift coefficient, $\frac{\text{Lift}}{qS}$
$C_m$	pitching-moment coefficient about the center of gravity, $\frac{\text{Pitching moment}}{qS\bar{c}}$

$\alpha$	angle of attack, deg
$C_{m\dot{\alpha}}$	rate of change of pitching-moment coefficient with angle of attack, $dC_m/d\alpha$
P	period of the short-period longitudinal oscillation, sec
$C_{mq} + C_{m\dot{\alpha}}$	pitch-damping parameter $\frac{\partial C_m}{\partial \frac{\dot{\theta}c}{2V}} + \frac{\partial C_m}{\partial \frac{\dot{\alpha}c}{2V}}$ per radian
$\dot{\theta}$	$\frac{d\theta}{dt}$ , radians/sec
$\dot{\alpha}$	$\frac{d\alpha}{dt}$ , radians/sec
$C_{L\dot{\alpha}}$	rate of change of lift coefficient with angle of attack $dC_L/d\alpha$ per degree
V	velocity, ft/sec
t	time, sec
$\theta$	flight-path angle
p	free-stream static pressure, lb/sq ft
$\rho$	density of air, slugs/cu ft
A	cross-sectional area, sq ft
l	model length from nose to fuselage base, 5.248 ft
x	distance measured rearward from the nose, ft
r	radius, ft
$a_l/g$	longitudinal accelerometer reading
$a_n/g$	normal accelerometer reading
$T_{1/2}$	time required for the short-period longitudinal oscillation to damp to one-half amplitude
$I_y$	mass moment of inertia of the model about the pitch axis (7.72 and 7.42 slug-ft <sup>2</sup> before and after sustainer rocket firing, respectively)

## MODEL AND APPARATUS

## Model

Figure 1 is a three-view drawing of the model used in this investigation; figure 2 shows total model cross-sectional area plotted against fuselage station; figures 3 to 5 are photographs of the model. The model had no duct inlet; the nose was faired to a point. The model was built basically of mahogany with steel and aluminum inserts and stiffeners. The nose was of Fiberglas laminations with heat-resistant plastic used as a bonding agent. The afterbody was cast aluminum. The body was built around a  $5\frac{1}{2}$ -inch-diameter steel tube which served to house the sustainer rocket motor and to secure the nose, wing, and tail. The wing and tail had steel and aluminum spars, respectively. The sustainer motor was a solid-fuel rocket developing about 3700-pounds thrust for 1 second and was used to accelerate the model from  $M = 1.30$  to  $M = 1.77$ .

Prior to flight-testing, the model was suspended by shock cords and excited in the vertical plane by an electromagnetic shaker. First- and second-bending and torsional natural frequencies of the wing were found to be 31, 101, and 256 cycles per second, respectively. First and second bending frequencies of the horizontal tail were found to be 94 and 298 cycles per second, respectively.

The horizontal tail was mounted at an angle of incidence of  $0^\circ$  with respect to the airplane center line, as was the wing.

Instrumentation consisted of a four-channel telemeter which transmitted continuous records of free-stream total pressure, model base pressure, normal acceleration, and longitudinal acceleration.

The model was equipped with two small rocket motors which served to disturb the model in pitch at preset times during the flight. These pulse rockets were located in the canopy, as can be seen in figure 3.

## Apparatus

The model was boosted to  $M = 1.30$  by a solid-fuel rocket motor developing an average thrust of 6000 pounds for 3 seconds. Data transmitted by the four-channel telemeter in the model were recorded by two ground receiving stations.

Throughout the flight, the model was tracked by two radar sets, one of which recorded position in space and the other recorded velocity of the model with respect to a ground reference point.

A radiosonde was used to determine atmospheric density, static pressure, and temperature throughout the altitude range traversed by the model flight. The radiosonde was tracked by radar to determine wind direction and velocity throughout the altitude range of the model flight.

#### METHOD OF ANALYSIS

All data reported herein were determined from the decelerating portions of the model flight where the model was separated from the booster and the sustainer rocket motor was not thrusting.

#### Drag

Total drag was determined by two independent methods. The first method consisted of differentiation with respect to time of the velocity (as determined from radar tracking), correcting for flight-path angle, and calculating total-drag coefficient by the relationship

$$C_{D_{total}} = -\left(\frac{dV}{dt} + 32.2 \sin \theta\right) \frac{W}{32.2qS}$$

The second method consisted of calculating drag coefficient by the relationship

$$C_{D_{total}} = -C_C = \frac{a_z}{g} \frac{W}{qS}$$

where  $\frac{a_z}{g}$  was determined directly from telemetered data and  $C_{D_{total}}$  was assumed equal to  $C_C$  since the model flew near zero lift.

Base drag was determined by the relationship

$$C_{D_{base}} = -\frac{(P_{base} - P)A_{base}}{qS}$$

Total drag coefficient by both methods was plotted and faired with equal weight on either method. Base drag was plotted and faired, and external drag was calculated from the relationship

$$C_{D_{external}} = C_{D_{total}} - C_{D_{base}}$$

## Lift

Lift was determined from the relationship

$$C_L = C_N = \frac{a_n}{g} \frac{W}{qS}$$

where  $\frac{a_n}{g}$  was determined directly from telemetered data, and  $C_L$  was assumed equal to  $C_N$  since the model flew near zero lift.

## Static Longitudinal Stability

Static longitudinal stability was determined through analysis of the short-period pitch oscillations which resulted from disturbances in pitch created by separation of the model from the booster, by "burnout" of the sustainer rocket, and by the two pulse-rockets. The relationship was

$$\frac{dC_m}{d\alpha} = C_{m\alpha} = \frac{-I_Y}{57.3qSc} \left[ \frac{4\pi^2}{P^2} + \left( \frac{0.693}{T_{1/2}} \right)^2 \right]$$

$$\frac{dC_m}{dC_L} = \frac{C_{m\alpha}}{C_{L\alpha}}$$

$$\frac{x_{ac}}{c} = \frac{x_{cg}}{c} - \frac{dC_m}{dC_L}$$

where  $C_{L\alpha}$  was obtained from references 1 and 2 (corrected for flexibility of this model) and  $T_{1/2}$  was determined from an analysis of the rate of decay of the pitch oscillations.

## Damping in Pitch

An analysis of the oscillations in pitch mentioned previously was used to determine values of time to damp to one-half amplitude  $T_{1/2}$

which, in turn, were used to determine nondimensional pitch-damping parameter from the relationship

$$C_{m_q} + C_{m_{\dot{\alpha}}} = \frac{\partial C_m}{\partial \frac{\dot{\theta}c}{2V}} + \frac{\partial C_m}{\partial \frac{\dot{\alpha}c}{2V}} = \frac{-8I_y}{\rho V S \bar{c}^2} \left[ \frac{0.693}{T_{1/2}} - \frac{C_{L_{\alpha}} \rho V S g}{4W} \right]$$

#### DISCUSSION OF RESULTS

The variation of Reynolds number with Mach number is shown in figure 6. Reynolds number varied from  $4.6 \times 10^6$  at  $M = 0.76$  to  $1.42 \times 10^6$  at  $M = 1.77$ . The center of gravity of the model was located 20 percent behind the leading edge of the mean aerodynamic chord.

#### Drag

Total drag is presented as a function of Mach number in figure 7. The curve has been faired with equal weight on telemeter and radar velocimeter data. Base drag is also shown in figure 7.

External drag, as determined from total and base drag is also presented in figure 7. The subsonic external drag coefficient is 0.012. The drag rise, based on  $\frac{dC_D}{dM} = 0.1$ , occurs at  $M = 0.95$ . The rise is rapid from a value of 0.016 at  $M = 0.95$  to 0.038 at  $M = 1.00$  and is followed by a gradual rise to a value of 0.043 at  $M = 1.20$ . Values of external drag, from references 1 and 2, are shown in figure 7 for comparison. Agreement between this test and the reference data shown appears to be good at subsonic speeds and fair at supersonic speeds. Estimates of skin-friction drag indicate that the wind-tunnel values of  $C_D$ , when corrected to the Reynolds numbers of the rocket-model test, decrease by about 0.002 at subsonic speeds and about 0.005 at supersonic speeds. This decrease would improve agreement except at the lowest subsonic speeds reported.

#### Longitudinal Trim

Figure 8 shows the variation with Mach number of trim lift coefficient. The trim change is mild and consists basically of a nose-up tendency at Mach numbers from 0.90 to 1.30 which is followed by a mild nose-down tendency to  $M = 1.72$ . Values from references 1 and 2,

corrected to the center-of-gravity location of this test, are shown for comparison. Agreement is good above  $M = 0.9$ .

### Longitudinal Stability

The period of the short-period pitch oscillation is shown in figure 9. The data point at  $M = 1.21$  (tailed symbol) was obtained prior to sustainer-rocket firing. Presented in figure 10 is static longitudinal stability  $C_{m\alpha}$  as determined from the values of pitch period presented in figure 9. In general, a slight decrease in static longitudinal stability from  $M = 1.03$  to  $M = 1.74$  is shown.

Lift-curve slope  $C_{L\alpha}$ , as determined from references 1 and 2, is presented in figure 11. The dashed curve in figure 11 includes an estimated correction for the flexibility of the model reported herein. In figure 12 is shown aerodynamic-center location as determined from figure 10 and the dashed curve of figure 11. In general, figure 12 indicates a mild forward movement of the aerodynamic center at Mach numbers from 1.03 to 1.74. Values from references 1 and 2 are also shown for comparison. The agreement is fair.

The time required for the short-period longitudinal oscillation to damp to one-half amplitude  $T_{1/2}$  is shown in figure 13. Figure 14 shows the pitch-damping parameter  $C_{mq} + C_{m\dot{\alpha}}$  per radian, as determined using  $T_{1/2}$  from figure 13 and  $C_{L\alpha}$  (flexible) from figure 11. Although the values of  $\frac{C_{m\dot{\alpha}}}{2V} + \frac{C_{mq}}{2V}$  are probably not directly applicable to the full-scale airplane because of the aeroelasticity mentioned previously, they indicate that damping is probably low at  $M = 1.03$  but increases to higher values at higher Mach numbers.

### FLUTTER AND BUFFET

There was an indication of mild wing flutter at Mach numbers between 0.94 and 1.11 at a frequency of 50 cycles per second (static first- and second-bending frequencies of the wing were 31 and 101 cycles per second, respectively, as mentioned previously). The amplitude of the oscillation was about 0.3g and was measured by the normal accelerometer which was located 5 inches outboard of the fuselage center line at about midchord. However, the full-scale airplane wing has approximately twice the scaled first-bending frequency as the model tested and, hence, will probably be free of flutter of this type.

There was no indication of buffet during any portion of the test reported herein.

### CONCLUSIONS

From this flight test of a 0.11-scale rocket model of the North American YF-100A airplane between Mach numbers of 0.76 and 1.77, the following conclusions are indicated:

1. The external drag coefficient varied from 0.012 at subsonic speeds to 0.043 at supersonic speeds. The drag-rise occurred at a Mach number of 0.95.

2. The low-lift longitudinal trim change was mild and consisted basically of a nose-up tendency at Mach numbers from 0.90 to 1.30 and was followed by a nose-down tendency to a Mach number of 1.72.

3. Damping in pitch was low at a Mach number of 1.03.

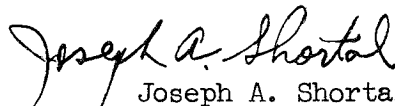
4. There was an indication of mild wing flutter at Mach numbers from 0.94 to 1.11. The full-scale airplane wing has approximately twice the scaled frequency as the model tested and, hence, will probably be free of this type of flutter. There was no indication of buffet during any portion of this investigation.

Langley Aeronautical Laboratory,  
National Advisory Committee for Aeronautics,  
Langley Field, Va.



Willard S. Blanchard, Jr.  
Aeronautical Research Scientist

Approved:



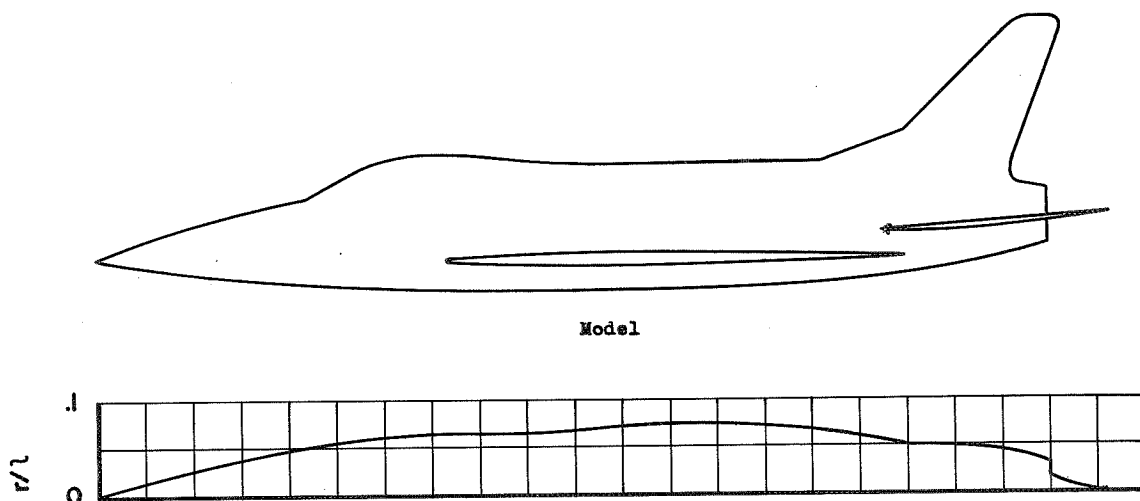
Joseph A. Shortal  
Chief of Pilotless Aircraft Research Division

fgs

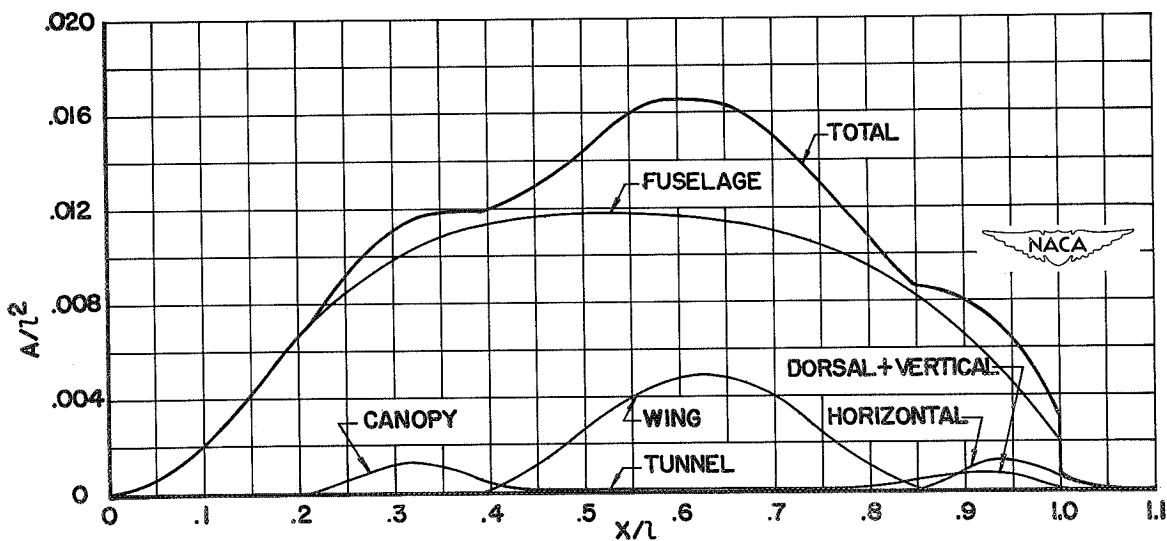
## REFERENCES

1. Mardin, H. R.: Supersonic Wind Tunnel Tests of the 0.02 Scale Full Span Model of the NA-180 (YF-100A) Airplane Through a Mach Number Range of 0.70 to 2.87 To Determine the Effect of Modifications to the Basic Model Components on the Aerodynamic Characteristics. Rep. No. SAL-43, North American Aviation, Inc., Oct. 30, 1952.
2. Safier, Irving: Report on Wind Tunnel Tests of a 0.07-Scale Sting-Mounted Model of the North American (Inglewood) F-100A (NA-180) Airplane at High Subsonic Speeds and  $M = 1.20$ . CWT Rep. 258, Southern Calif. Cooperative Wind Tunnel, Sept. 4, 1952.





(a) Equivalent body of revolution (complete model).



(b) Breakdown of areas of the components.

Figure 2.- Area distribution of the model tested.

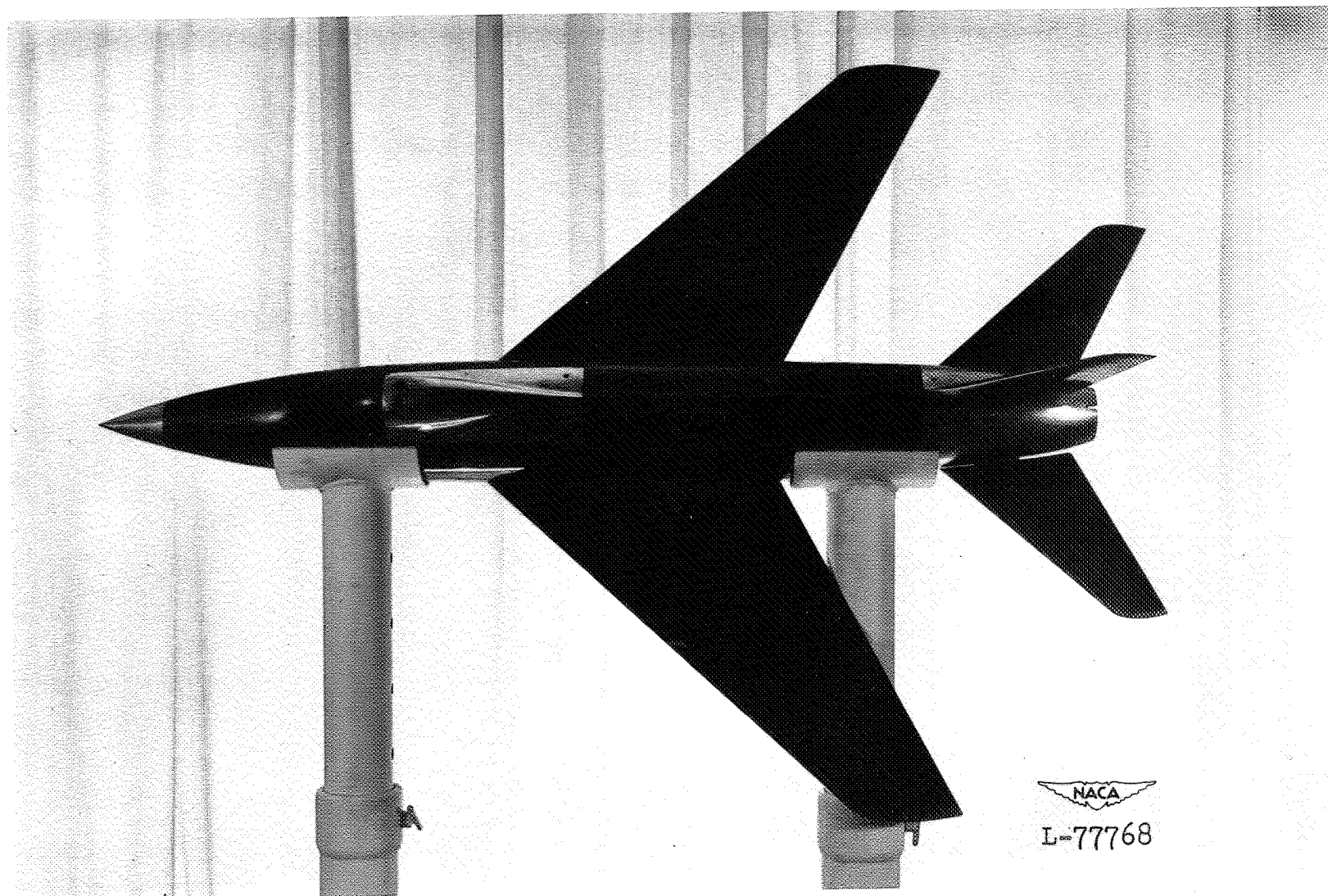


Figure 3.- Top view of model tested.

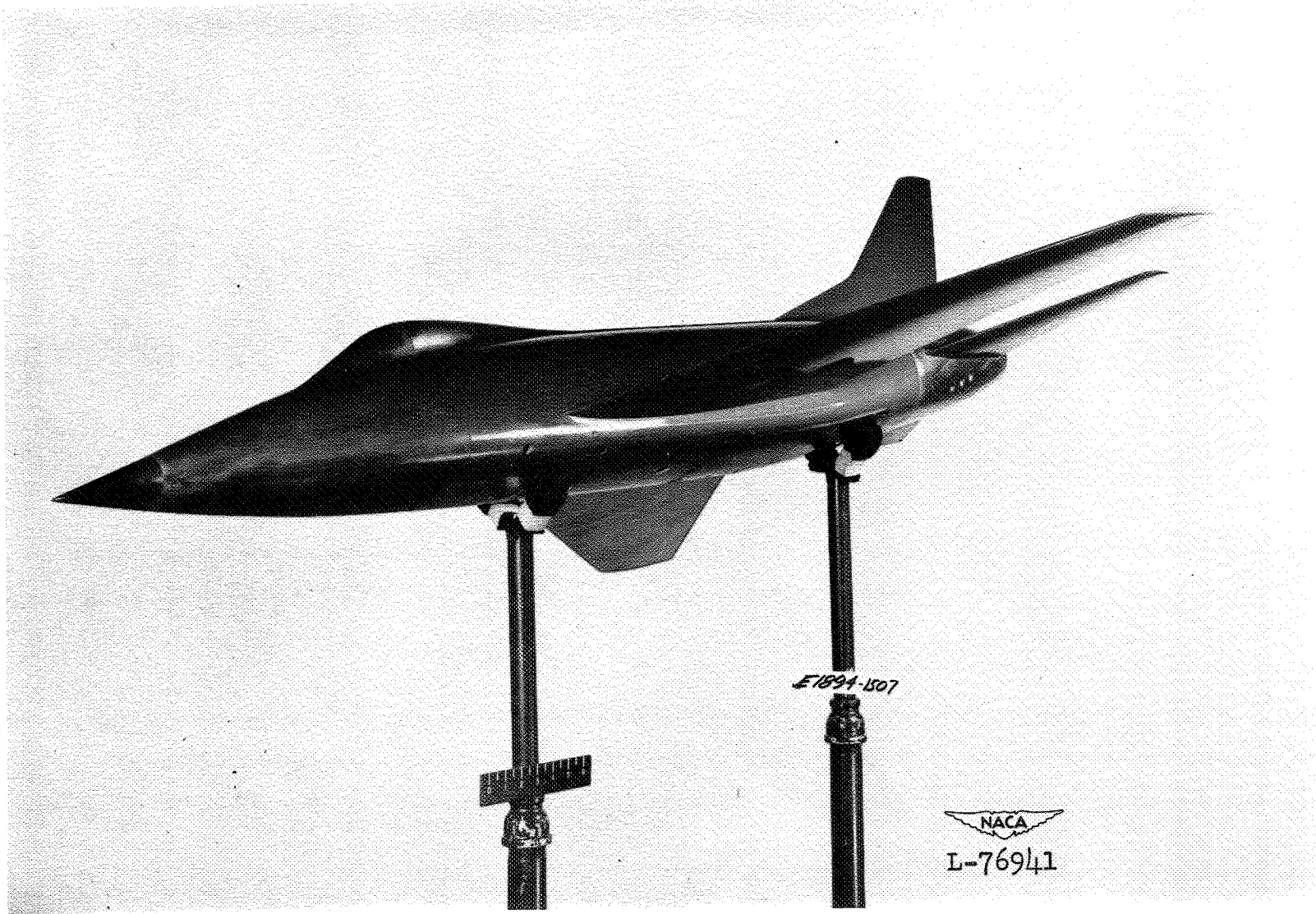


Figure 4.- Three-quarter front view.

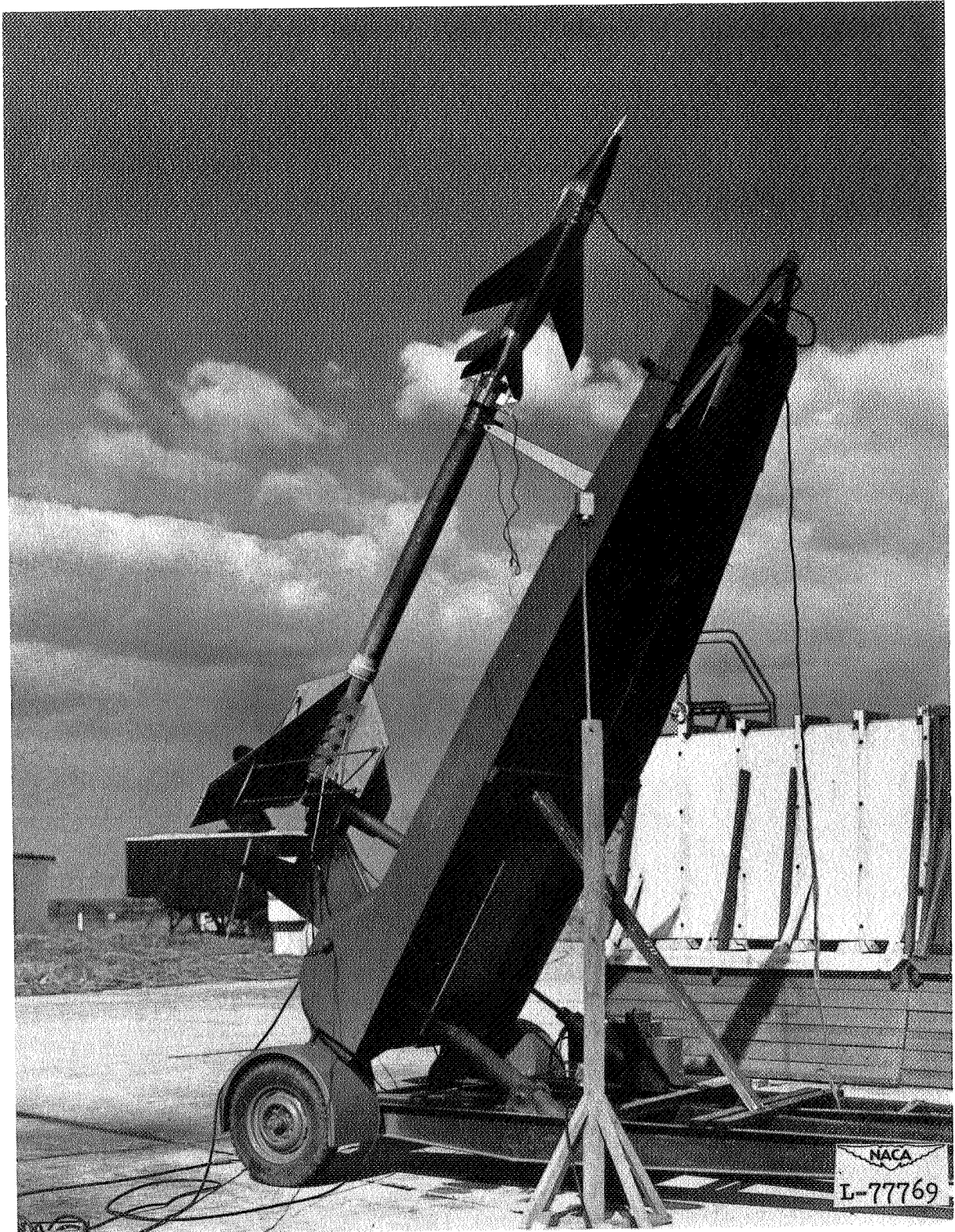


Figure 5.- Booster-model combination in launching position.

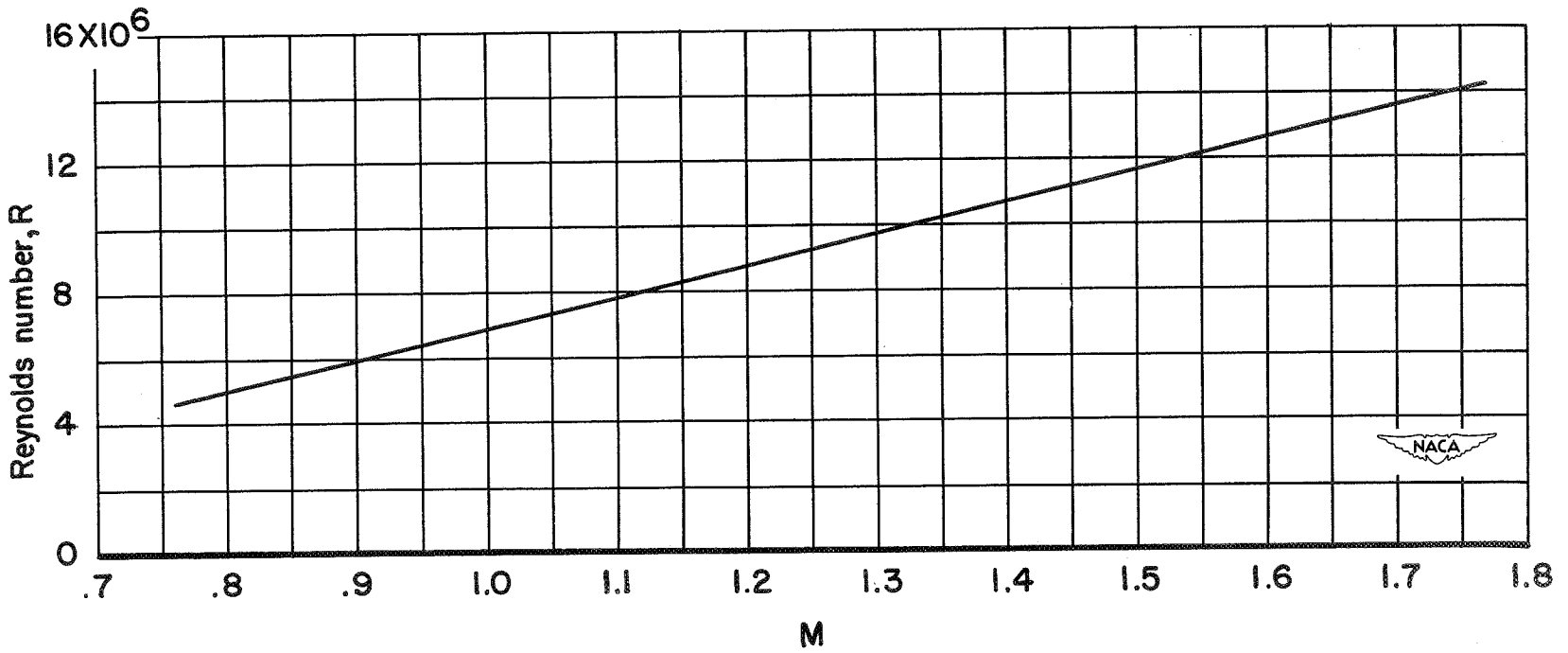


Figure 6.- Variation of Reynolds number with Mach number.

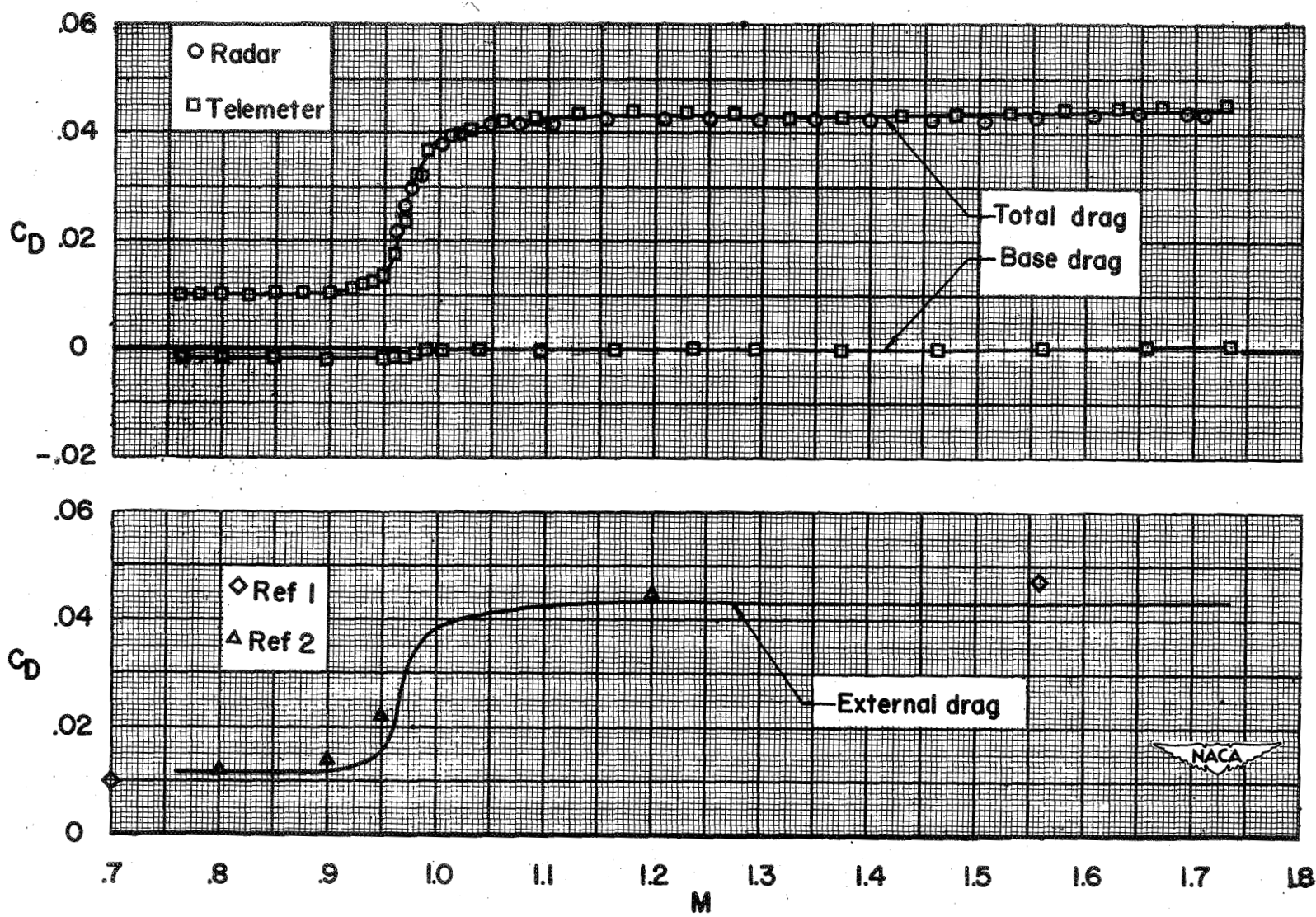


Figure 7.- Drag.

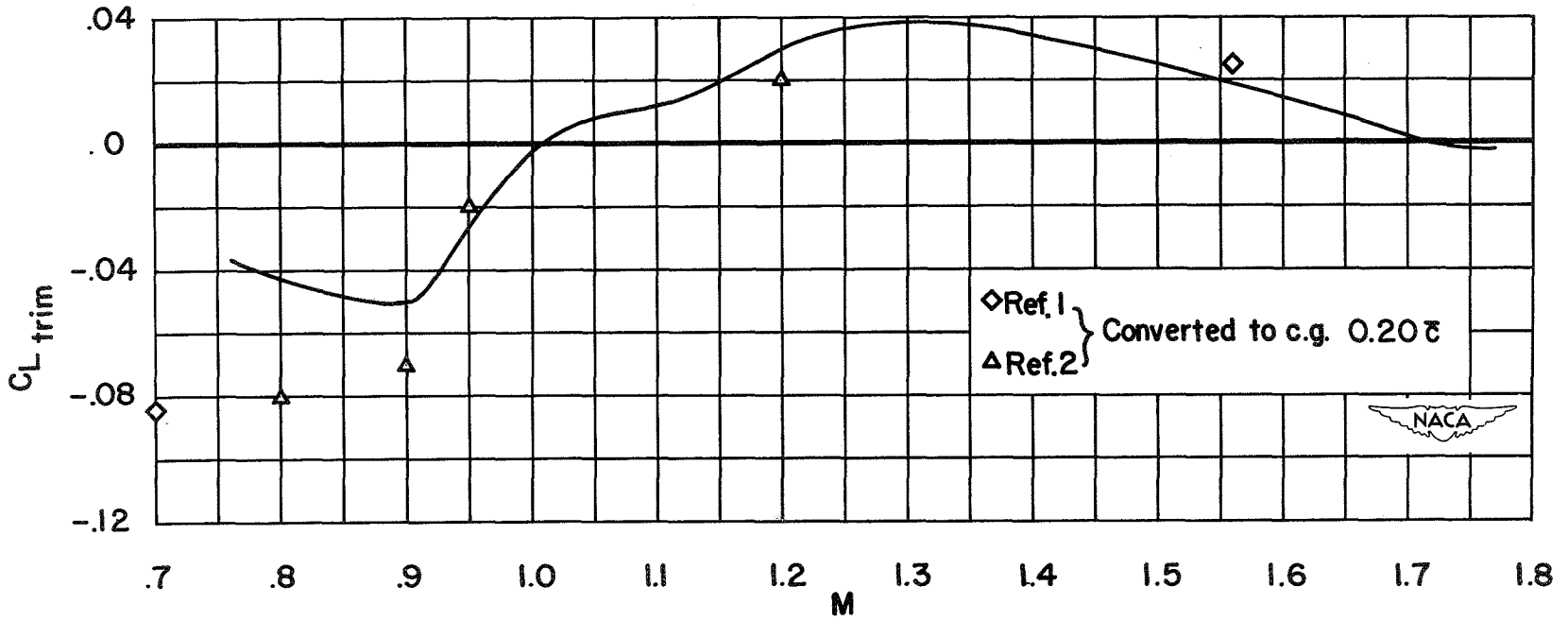


Figure 8.- Trim-lift.

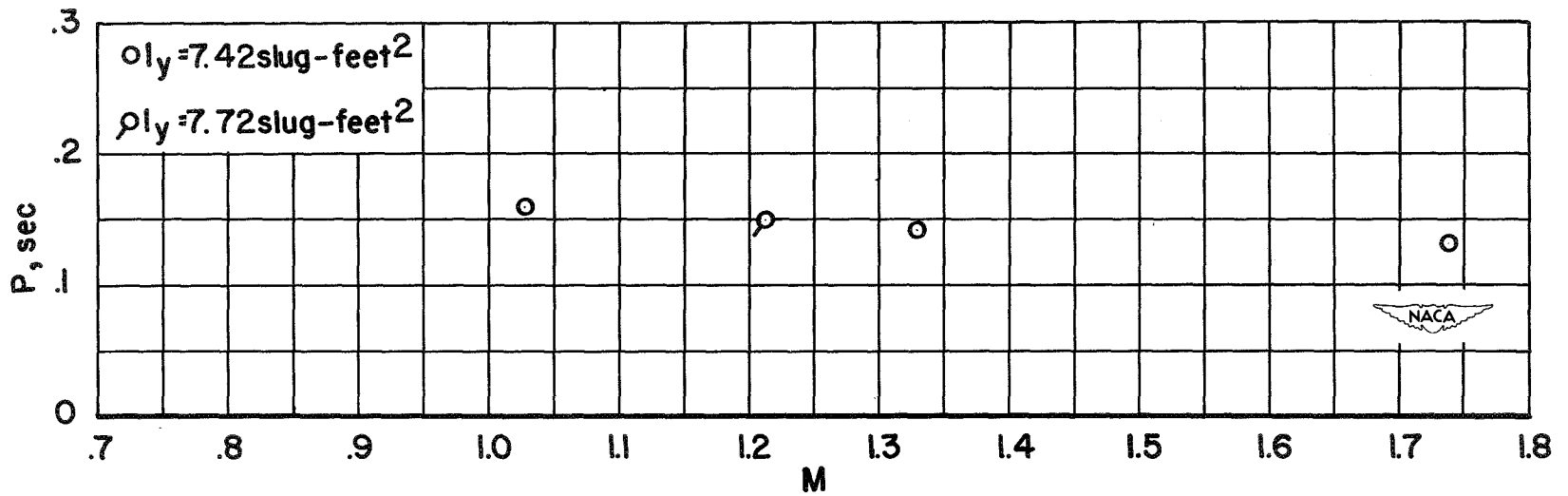


Figure 9.- Period of the short-period longitudinal oscillation.

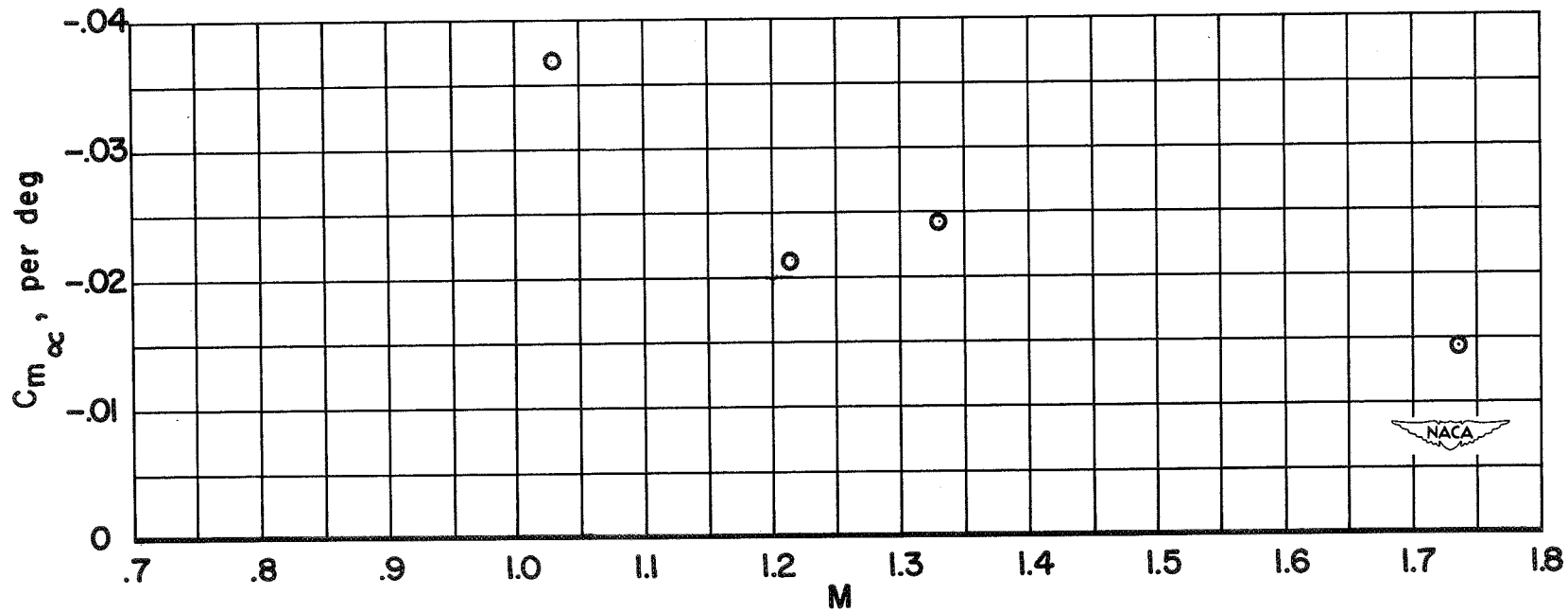


Figure 10.- Static longitudinal stability.

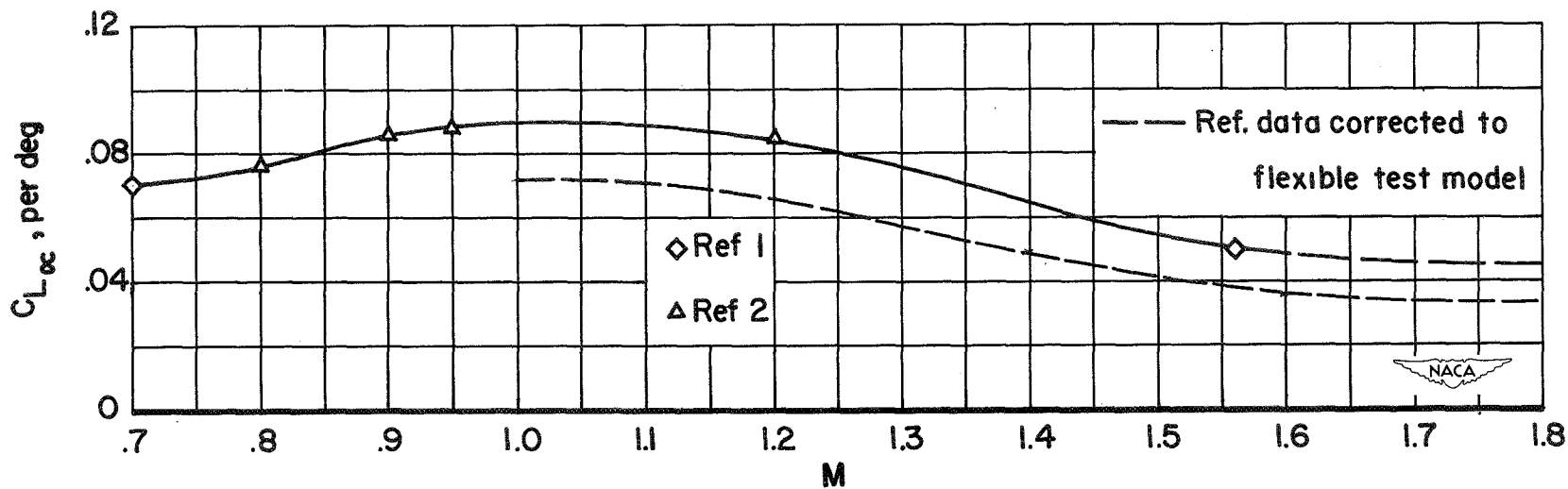


Figure 11.- Lift-curve slope (from refs. 1 and 2).

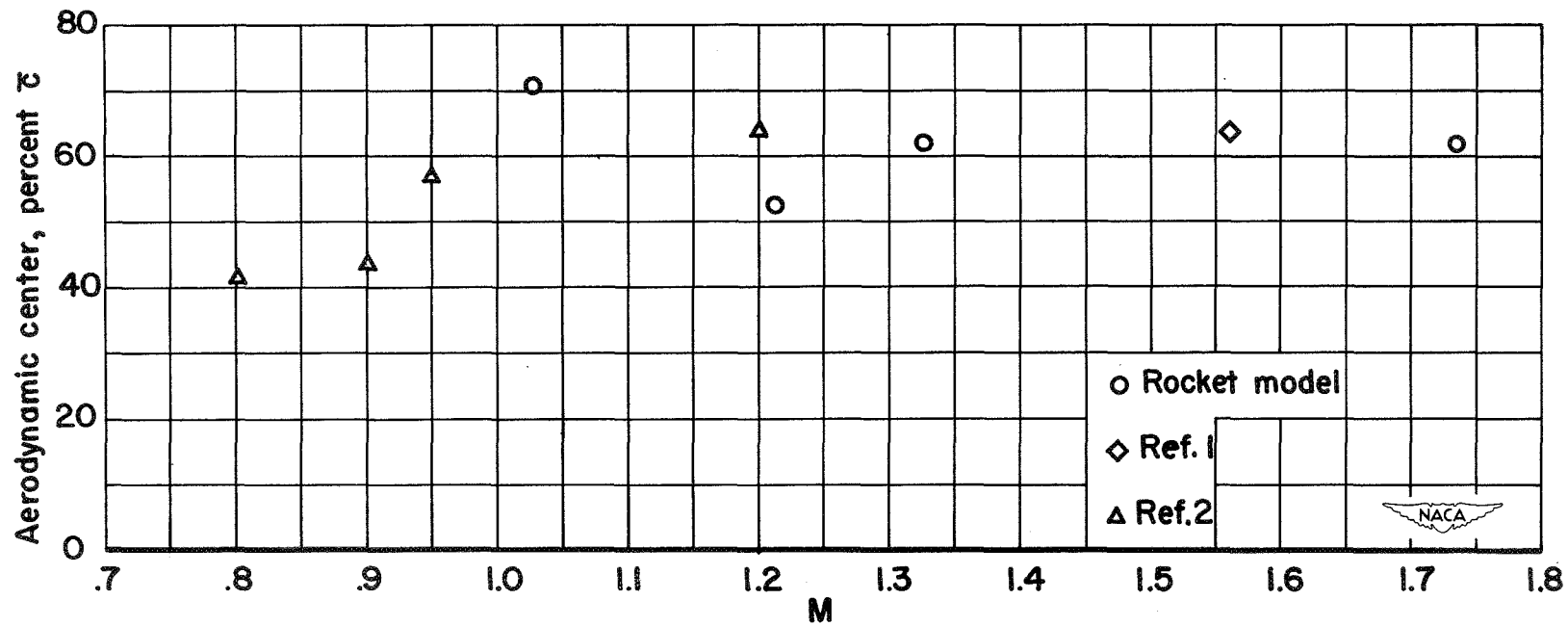


Figure 12.- Aerodynamic-center location.



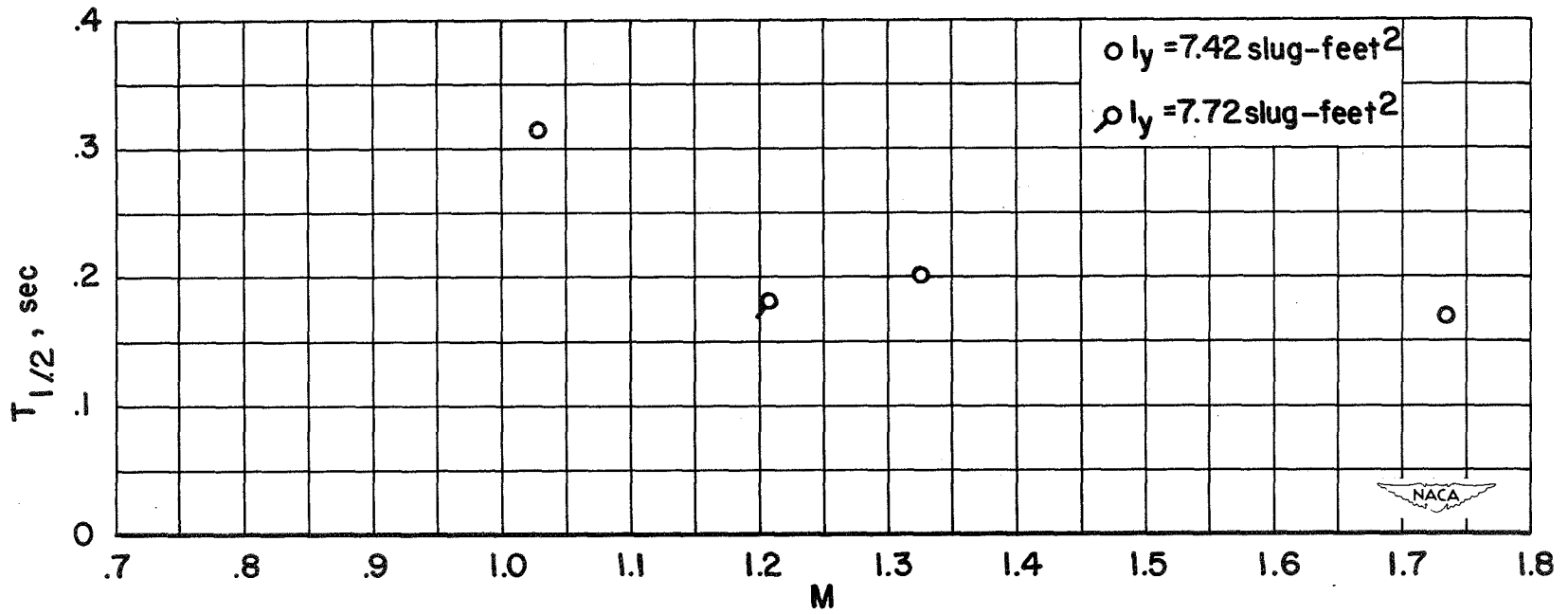


Figure 13.- Time required for the short-period longitudinal oscillation to damp to one-half amplitude.

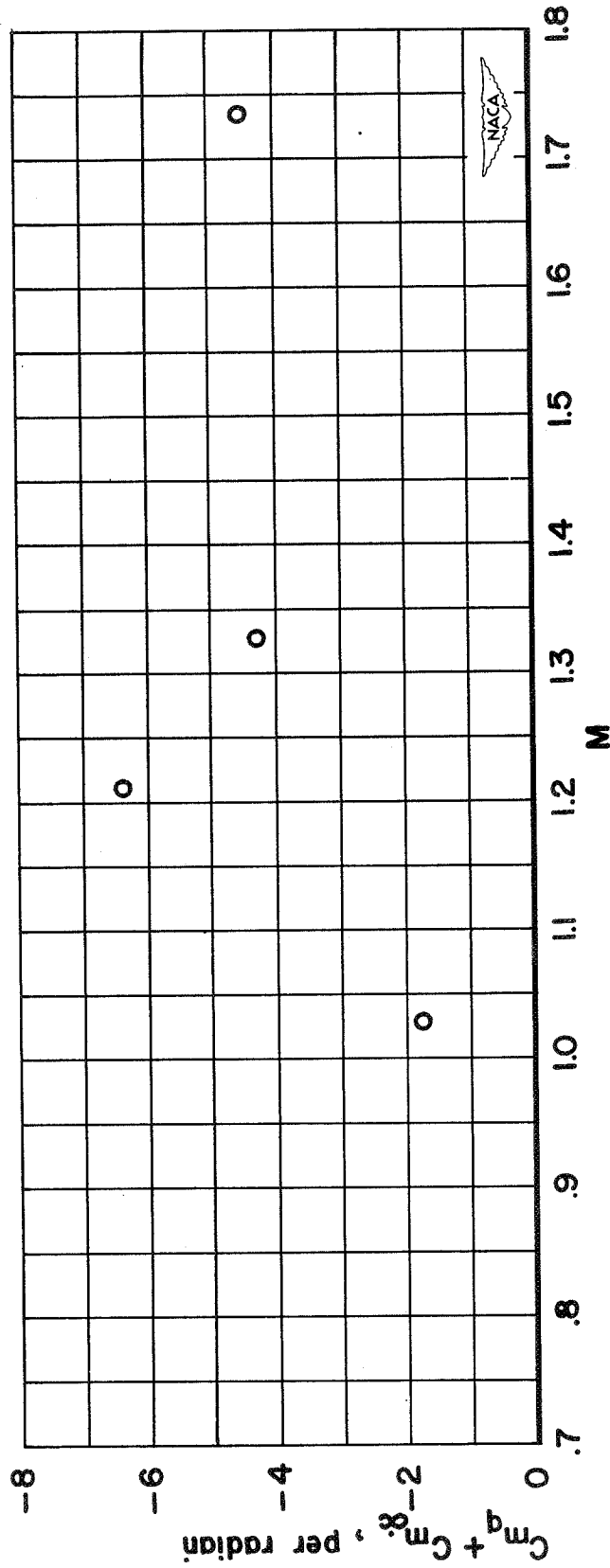


Figure 14.- Pitch-damping parameter.